Published in final edited form as:
J Biol Rhythms. 2011 June ; 26(3): 200–209. doi:10.1177/0748730411401740.

Effects of Vasoactive Intestinal Peptide Genotype on Circadian Gene Expression in the Suprachiasmatic Nucleus and Peripheral Organs

Dawn H. Loh[*], **Joanna M. Dragich**[*,1], **Takashi Kudo**[*], **Analyne M. Schroeder**[*], **Takahiro J. Nakamura**[*,2], **James A. Waschek**[*], **Gene D. Block**[*], and **Christopher S. Colwell**[*,3]

[*]Department of Psychiatry and Biobehavioral Sciences, University of California–Los Angeles, Los Angeles, CA

Abstract

The neuropeptide vasoactive intestinal polypeptide (VIP) has emerged as a key candidate molecule mediating the synchronization of rhythms in clock gene expression within the suprachiasmatic nucleus (SCN). In addition, neurons expressing VIP are anatomically well positioned to mediate communication between the SCN and peripheral oscillators. In this study, we examined the temporal expression profile of 3 key circadian genes: *Per1*, *Per2*, and *Bmal1* in the SCN, the adrenal glands and the liver of mice deficient for the *Vip* gene (VIP KO), and their wild-type counterparts. We performed these measurements in mice held in a light/dark cycle as well as in constant darkness and found that rhythms in gene expression were greatly attenuated in the VIP-deficient SCN. In the periphery, the impact of the loss of VIP varied with the tissue and gene measured. In the adrenals, rhythms in *Per1* were lost in VIP-deficient mice, while in the liver, the most dramatic impact was on the phase of the diurnal expression rhythms. Finally, we examined the effects of the loss of VIP on ex vivo explants of the same central and peripheral oscillators using the PER2::LUC reporter system. The VIP-deficient mice exhibited low amplitude rhythms in the SCN as well as altered phase relationships between the SCN and the peripheral oscillators. Together, these data suggest that VIP is critical for robust rhythms in clock gene expression in the SCN and some peripheral organs and that the absence of this peptide alters both the amplitude of circadian rhythms as well as the phase relationships between the rhythms in the SCN and periphery.

Keywords

adrenal gland; bioluminescence; *Bmal1*; circadian; liver; neuropeptides; *Per1*; *Per2*; suprachiasmatic nucleus; VIP

Daily rhythms in behavior and physiology are well documented in a large variety of species and, in mammals, are ultimately coordinated by the SCN in the hypothalamus (Moore and Eichler, 1972; Hastings et al., 2003; Dibner et al., 2010). Embedded within a circuit, SCN neurons generate robust, synchronized rhythms of clock gene expression, while in isolation, these same neurons generate low amplitude, variable circadian oscillations (Yamaguchi et al., 2003; Aton et al., 2004; Liu et al., 2007; Webb et al., 2009). While a number of

[3]To whom all correspondence should be addressed: Department of Psychiatry and Biobehavioral Sciences, University of California–Los Angeles, 760 Westwood Plaza, Los Angeles, CA 90024-1759; ccolwell@mednet.ucla.edu. .
[1]Present address: Department of Neurology, Columbia University, 650 West 168th Street, New York City, NY 10032.
[2]Present address: Faculty of Pharmaceutical Sciences, Teikyo Heisei University, 4-1 Uruidominami, Ichihara, Chiba 290-0193, Japan.

mechanisms are known to mediate communication between SCN neurons (Welsh et al., 2010), the neuropeptide VIP has emerged as the leading candidate molecule responsible for intercellular synchronization within the SCN. We and others have hypothesized that VIP acts as either a neurotransmitter or paracrine factor that mediates communication within the SCN (Harmar et al., 2002; Colwell et al., 2003; Piggins and Cutler, 2003; Aton et al., 2005; Maywood et al., 2006; Vosko et al., 2007; Ciarleglio et al., 2009).

At the behavioral level, all of the mice deficient in VIP or its receptor ($VPAC_2R$) exhibit severe disruptions in their ability to express a coherent circadian rhythm in constant conditions (Harmar et al., 2002; Colwell et al., 2003). In many cases, the transgenic mice exhibit wheel-running behavior that is arrhythmic on the circadian time scale, while other mutant mice express a rhythm with a significantly shortened period lacking in coherence and statistical power due to variability in activity onset and expansion of the duration of wheel-running activity. At the physiological level, the loss of VIP or $VPAC_2R$ results in poorly synchronized SCN neurons (Aton et al., 2005; Ciarleglio et al., 2009), which ultimately reduces the amplitude of the rhythms generated by the SCN as a population (Brown et al., 2007; Ciarleglio et al., 2009). At the molecular level, the loss of VIP or the $VPAC_2R$ causes the loss of the rhythm in *Per1*-driven GFP or luciferase reporters due to the loss of the synchronization of the cellular oscillators (Maywood et al., 2006; Hughes et al., 2008; Ciarleglio et al., 2009). In $VPAC_2R$-deficient mice, the in vivo gene expression rhythms in *Per1*, *Per2*, and *Bmal1* are also highly attenuated (Harmar et al., 2002), which suggests the importance of VIP and its receptor on rhythms in clock gene expression in the SCN. In addition, outputs from the SCN govern a host of downstream daily rhythms (Hastings et al., 2003; Dibner et al., 2010), and VIP is also found in many of the SCN efferents projecting to the paraventricular nucleus (PVN) (Teclemariam-Mesbah et al., 1997; Buijs et al., 1999). Previous work has found that VIP-deficient mice lose their circadian rhythms in corticosterone (Loh et al., 2008) as well as in heart rate (Schroeder et al., 2011). Therefore, we would predict an impact of the loss of VIP on clock gene expression not only in the SCN but also in the peripheral organs.

To examine the role of VIP in the circadian timing loop, we performed gene expression analyses of 3 key components of the molecular oscillator: *Per1* as an indicator of immediate-early gene action, and *Per2* and *Bmal1* (also known as *Arntl*) as antiphase components of the interlinked transcription/translation feedback loop at the core of the molecular oscillator. To determine the necessity of VIP for the normal functioning of the molecular oscillator in the master pacemaker, we examined the expression of these genes in the SCN of VIP-deficient mice using in situ hybridization (ISH). We also examined the expression of these same genes in 2 peripheral organs with well-characterized circadian oscillations using real-time reverse transcriptase polymerase chain reaction (RT-PCR): the adrenal glands and liver. Finally, we examined the effects of the loss of VIP on ex vivo explants of the SCN, adrenals, and liver using the PER2::LUC reporter system, where we could make a clearer comparison of the amplitude and phases of the measured rhythms.

MATERIALS AND METHODS

Animals

The experimental protocols used in this study were approved by the UCLA Animal Research Committee, and all recommendations for animal use and welfare, as dictated by the UCLA Division of Laboratory Animals and the guidelines from the National Institutes of Health, were followed. The ISH and real-time RT-PCR experiments used 3- to 6-month-old $Vip^{+/+}$ (WT) and $Vip^{-/-}$ (VIP KO; also deficient in peptide histidine isoleucine [PHI] due to coding by the same locus) littermates on a C57BL/6 background from our colony (minimum of 12 generations backcrossed) (Colwell et al., 2003), with supplementation by WT mice

from the same colony when necessary. To perform real-time ex vivo monitoring of PER2::LUC-driven bioluminescence rhythms, we crossed PER2::LUC knock-in mice on a C57BL/6J background (Yoo et al., 2004) with the *Vip*$^{-/-}$ line and maintained the line as homozygotes for the PER2::LUC knocked-in fusion gene.

Lighting Conditions

All mice were entrained to 12:12 LD conditions for a minimum of 2 weeks prior to any manipulations. For tissue collections performed under LD, mice were sacrificed according to zeitgeber time (ZT). For tissue collections performed under DD, mice were initially entrained to 12:12 LD conditions for at least 2 weeks, followed by between 4 to 7 days of DD conditions. To calculate circadian time (CT), a best-fit line was drawn through the daily onset of wheel-running activity (defined as CT 12) to determine the free-running period of each animal.

ISH

ISH of 20-μm coronal SCN sections was performed as previously described (Dragich et al., 2010) using plasmids (pCRII, Invitrogen, Carlsbad, CA) containing the cDNA for *Per1* (340-761 nt, accession number AF022992, generously provided by Dr. D. Weaver, University of Massachusetts), *Per2* (9-489 nt, accession number AF035830), and *Bmal1* (864-1362 nt, accession number AB015203). Riboprobes were synthesized, and ISH was performed on 20-μm coronal sections containing the SCN, and each run was performed on all time points of both genotypes as previously described (Wang et al., 2009; Dragich et al., 2010).

Real-Time RT-PCR

Real-time RT-PCR was performed as previously described (Dragich et al., 2010) using the SYBR Green Master Mix (Applied Biosystems, Foster City, CA). Primers for *Per1* (sense: 5′-TCC TCC TCC TAC ACT GCC TCT-3′ and anti-sense: 5′-TTG CTG ACG ACG GAT CTT T-3′), *Per2* (sense: 5′-GGG CAT TAC CTC CGA GTA TA-3′ and anti-sense: 5′-GGC GAC TTG GTT GGA GAT GTA-3′), *Bmal1* (sense: 5′-GCA AAC TAC AAG CCA ACA TTT C-3′ and anti-sense: 5′-TTC CCT CGG TCA CAT CCT AC-3′), and *Actb* (sense: 5′-CCA ACC GTG AAA AGA TGA CC-3′ and anti-sense: 5′-CCA GAG GCA TAC AGG GAC AG-3′) were designed to cross intron-exon boundaries. Primer specificity and efficiency were confirmed, and no-RT controls were run routinely. Each run of the quantitative PCR was performed on all time points of both genotypes along with a standard curve as previously described (Dragich et al., 2010). The expression levels of *Per1*, *Per2*, and *Bmal1* transcripts were determined using the $2^{-\Delta\Delta Ct}$ method, using *Actb* as the normalizing reference gene. We confirmed that the levels of *Actb* did not vary with the daily cycle in the adrenal glands and liver.

Real-Time Monitoring of Bioluminescence by a Photomultiplier Tube Photodetector

Ex vivo explants of the SCN, adrenal glands, and liver from WT; PER2::LUC and VIP KO; and PER2::LUC mice were prepared between ZT 10 to ZT 11 from mice housed in a 12:12 LD cycle, with the explants entering the Lumicycle photometer (Actimetrics, Wilmette, IL) no later than ZT 12. Dissection and culture guidelines as recommended by Yamazaki and Takahashi (2005) were followed. For SCN explants, 300-μm coronal sections were prepared using a vibratome (Dosaka EM, Kyoto, Japan), and the paired SCN (~1 mm^2) was then selectively dissected from the rest of the coronal slice with 2 cuts using sterile scalpels. Liver explants (1-2 mm^3) were obtained by a single cut from the median lobe using sterile scissors, and halved adrenal explants were obtained by performing a single cut with a sterile scalpel. The prepared explants were transferred onto Millicell membranes (0.4 μm,

PICMORG50, Millipore, Bedford, MA) resting on 1.2 mL of recording media (Yamazaki and Takahashi, 2005) that contained freshly added 0.1 mM luciferin (sodium salt monohydrate, Biosynth, Staad, Switzerland), and the 35-mm dishes were sealed using autoclaved high-vacuum grease (Dow Corning, Midland, MI). The explants were monitored at 37 °C for 7 to 10 consecutive uninterrupted days, and the raw bioluminescence values were normalized by first subtracting the recorded baseline, then subtracting a running average of 24 hours of this baseline-subtracted bioluminescence, and finally performing a 2-hour smoothing average. Period was calculated from an average of no less than 6 peak-to-peak times. Amplitude was calculated by summing the peak and subsequent trough values. Rate of amplitude damping was calculated from the slope of no less than 6 consecutive amplitudes using the following formula: $y = ae^{bx}$, where **x** indicates the number of days to "damp" for the value of **y** (amplitude) that is 1/*e* of the first amplitude, **a** is the intercept of the exponential regression through amplitude versus time, and **b** is the **x** variable coefficient. We report the **x** value of days to damp as the indicator of damping in our results. Due to using a 24-hour moving average as a normalizing factor, we could not use the first actual recorded peak to determine the phase of the explants and instead refer to the second recorded peak (or first calculated peak) as the first peak for phase relationships in the results. Variability of peak-to-peak timing was calculated using the standard deviation between no less than 6 recorded peaks for each sample as another indicator of instability of the molecular oscillator.

Statistical Analysis

One-way analysis of variance (ANOVA) was applied to the data from the ISH and RT-PCR experiments to determine the presence of differences in gene expression over time. Post hoc Holm-Sidak test was applied to determine peak and trough times of expression. To determine effects of ZT and genotype, we applied 2-way ANOVA followed by the Holm-Sidak post hoc test. Student *t* tests were used to compare the amplitude (peak to trough ratio) of transcript expression and the parameters of the bioluminescence recordings. All results were reported to be significantly different if $p < 0.05$ (*p* values reported where possible unless < 0.001). All tests were performed using SigmaStat (version 3.5, SYSTAT Software, San Jose, CA). Values are shown as mean ± standard error of the mean (SEM).

RESULTS

Diurnal Profile of Gene Expression in the SCN, Adrenal Glands, and Liver of VIP KO Mice

Per1 transcript expression in the SCN was examined in WT and VIP KO mice housed under LD conditions using ISH (Fig. 1A and Table 1). While WT mice displayed clear rhythms in *Per1* expression with a peak at ZT 6, VIP KO mice did not exhibit a diurnal rhythm. Although no significant peak-to-trough difference could be determined by post hoc analysis for *Per1* expression in VIP KO SCN, we compared the highest mean value to the lowest mean value to determine the amplitude for this and subsequent data sets and found it to be significantly decreased in the VIP KO. Expression of *Per1* in the adrenal glands and liver was examined by real-time RT-PCR and was confirmed to be rhythmic in WT samples. The adrenal glands of VIP KO mice failed to show any diurnal rhythm in *Per1* expression, but a faint rhythm of expression was still observed in the liver, albeit with a reduced amplitude and a shift in peak phase to ZT 2.

We also measured diurnal rhythms in *Per2* expression in the SCN, adrenal glands, and liver of WT mice (Fig. 1B and Table 1). We found a lack of rhythmic expression of *Per2* in VIP KO SCN as well as a reduction in the peak-to-trough difference of expression. The adrenals glands of VIP KO mice also failed to display a significant rhythm in *Per2* expression. In the

liver, *Per2* expression in the VIP KO remained rhythmic but with a shift in the phase of peak expression to ZT 10.

The final gene examined, *Bmal1*, also showed clear diurnal rhythms of expression in the SCN, adrenal glands, and liver of WT mice (Fig. 1C and Table 1). There was no diurnal variation in *Bmal1* expression in the SCN from VIP KO mice. In contrast, the adrenal glands of VIP KO mice showed a diurnal rhythm in *Bmal1* expression, although the amplitude was reduced and the phase of peak expression was shifted to ZT 18. A diurnal rhythm persisted in the liver of VIP KO, also with a shift in the phase of peak expression.

Circadian Profile of Gene Expression in the SCN, Adrenal Glands, and Liver of VIP KO Mice

The expression of the *Per1* transcript in the SCN, adrenal glands, and liver was examined in WT and VIP KO mice housed under DD conditions. We confirmed circadian rhythms in the expression of *Per1* in WT SCN, adrenal, and liver samples (Fig. 2A and Table 2) and found a much reduced amplitude rhythm in the SCN from VIP KO mice. *Per1* expression in the adrenals did not show any sign of circadian variation in the VIP KO mice. In the liver, there was no significant rhythm in *Per1* expression, although the expression profile appears to be shifted in phase.

Circadian rhythms in *Per2* expression were also confirmed in WT samples (Fig. 2B and Table 2). Although no rhythm in *Per2* expression was detected in VIP KO SCN, we observed rhythms in the adrenal glands and liver. The timing of peak expression was altered in the VIP KO adrenal glands, and there was no difference in peak-to-trough amplitude of *Per2* expression in either the adrenal glands or liver.

Rhythmic *Bmal1* expression was confirmed in WT SCN, adrenal glands, and liver (Fig. 2C and Table 2). There was no rhythm in *Bmal1* expression in the SCN of VIP KO mice, and the peak-to-trough amplitude was reduced. *Bmal1* was rhythmic in both the adrenal glands and liver of VIP KO mice with slightly reduced amplitudes of peak-to-trough expression. A secondary peak in *Bmal1* expression was observed in the subjective day of both peripheral organs examined.

PER2-Driven Luciferase Activity in the SCN, Adrenal Glands, and Liver of VIP KO Mice

Finally, we generated mice doubly transgenic for the VIP KO and the PER2::LUC knock-in so as to follow the amplitude and phase of each tissue over time (Fig. 3A). In the SCN explants, the parameter most dramatically reduced in the VIP KO was amplitude of the first peak (Fig. 3A and 3B and Table 3). The period, phase of the first calculated peak (Fig. 3C), and rate at which amplitude damped were not found to be different between WT and VIP KO SCN explants (Table 3). The peak-to-peak variability of the VIP KO explants, as measured by the standard deviation of the time interval between peaks (Table 3), was significantly greater than the WT controls. In the adrenal explants, the most altered parameter was the phase of the first calculated peak (Fig. 3C), with the VIP KO adrenals showing a phase advance in the timing of the peak compared to WT adrenals. No changes in the period, amplitude, rate of damping, and peak-to-peak variability were found in VIP KO adrenal explants (Table 3). The liver explants displayed a similar phenotype, with a phase advance in the first calculated peak of VIP KO liver (Fig. 3C) compared to the WT controls. Like the adrenals, the period, amplitude, and damping rate of the VIP KO liver explants were not altered (Table 3). The peak-to-peak variability of the VIP KO liver explants, however, was significantly greater than the WT controls. In summary, the rhythms in PER2::LUC-driven luciferase activity continue in the SCN, adrenal glands, and liver of VIP KO mice. However, the amplitude of the SCN rhythm is greatly reduced, and the phase

relationship between the 3 studied tissues is altered, with both adrenal glands and liver showing a phase advance in the first peak.

DISCUSSION

In this study, we investigated how the diurnal and circadian rhythms in the molecular clock within the SCN and its peripheral targets are altered by the loss of VIP. We found that the diurnal expression patterns of *Per1*, *Per2*, and *Bmal1* were no longer rhythmic in the SCN of VIP KO mice. Under DD, a low amplitude rhythm was detected in *Per1* expression, while no rhythms of *Per2* and *Bmal1* expression were observed in the SCN of VIP KO mice. Using ex vivo bioluminescence monitoring of PER2::LUC-driven luciferase activity in $Vip^{-/-}$ double transgenic mice, we found that the period, phase, and damping of the VIP KO SCN explants were not altered but that the amplitude of the rhythm was severely blunted, and there was an increase in cycle-to-cycle variability in the phase of peak expression. We conclude from these findings that the SCN requires normal VIP expression to express robust rhythms in *Per1*, *Per2*, and *Bmal1* transcripts.

The aberrant expression rhythms in these core clock genes largely agree with the prior work with $VPAC_2R$ KO mice where rhythmic expression of *Per1*, *Per2*, and *Cry1* was found to be greatly reduced (Harmar et al., 2002). Later work in which the $VPAC_2R$ mice were crossed into bioluminescence reporter lines with the *Per1* promoter driving either GFP or luciferase found that expression was still rhythmic but at a very low amplitude and also with variable cycle length (Maywood et al., 2006). While we did not measure expression patterns from single cells, the results from prior work using the $VPAC_2R$-deficient *Per1*::GFP (Maywood et al., 2006; Hughes et al., 2008) as well as VIP-deficient *Per1*::GFP lines (Ciarleglio et al., 2009) all suggest that the loss of rhythmicity at the population level is due to the loss of synchrony among the single-cell oscillators within the SCN population. Electrical recordings from individual SCN neurons (Aton et al., 2005) also indicate that the loss of synchronization of the cellular oscillators is at least part of the reason that the neural activity rhythm in the population is lost (Brown et al., 2007). Single SCN neurons appear to be unstable circadian oscillators (Webb et al., 2009), and our results are broadly consistent with the proposed role for VIP as a coupling agent within the SCN that stabilizes these single-cell oscillations.

The behavioral deficits of the VIP-deficient mice have already been described in past studies (Colwell et al., 2003; Aton et al., 2005; Vosko et al., 2007; Ciarleglio et al., 2009; Power et al., 2010), and we did not focus on this aspect of the phenotype of the mutant mice in the present work. Nevertheless, it is interesting to note that the wheel-running behavior of the VIP-deficient mice was still rhythmic when we sacrificed the mice in DD. In fact, we only used mutant mice in which we were able to clearly pick out activity onset in order to estimate CT 12. This does raise the question of how the VIP KO mice were able to exhibit a coherent, albeit abnormal, behavioral rhythm without distinct rhythms in gene expression in the SCN. Another interesting aspect of these results is that we found that the phase of the SCN oscillation of PER2::LUC was not significantly phase advanced compared to WT controls. Behaviorally, all of the VIP-deficient mice exhibit a very positive phase angle when released into DD such that their activity starts 6 to 8 hours before the time of the prior lights-off, while WT mice may start activity less than 1 hour before the time of the prior lights-off. Entrainment mechanisms are clearly altered in the VIP-deficient mice (Colwell et al., 2003), which among other deficits, show a greatly reduced light induction of c-FOS and *Per1* in the SCN (Dragich et al., 2010). Our present data suggest that this phase advance in entrainment is not simply due to an advance in the molecular oscillator but that a more complex underlying reason exists. The optical measurements of PER2::LUC rhythms agreed with our in vivo findings that the main deficit lies in the amplitude of the oscillation, and

while more variable in the mutants, the phase of the SCN PER2::LUC rhythms did not vary between the genotypes. Modeling studies of the molecular oscillator in the SCN suggest that low amplitude rhythms are much more susceptible to agents that cause phase shifts (Vitaterna et al., 2006; Brown et al., 2008), which is another mechanism that may explain the abnormal behavioral phase angle observed in the VIP mutants.

The necessity of the SCN for coordination of a host of peripheral rhythms has repeatedly been demonstrated by lesions of the SCN (Guo et al., 2005) and forebrain-specific circadian gene ablation studies (McDearmon et al., 2006). Anatomical studies have provided evidence that the PVN receives VIP-positive innervations from the SCN (Mezey and Kiss, 1985; Teclemariam-Mesbah et al., 1997; Kalló et al., 2004). The PVN neurons send projections throughout the central nervous system and endocrine system, providing multiple pathways by which the SCN can convey temporal information to the brain and body, with the autonomic nervous system and the hypothalamic-pituitary-adrenal axis thought to be critical outputs (Buijs et al., 1999; Kalsbeek et al., 2006). Furthermore, transneuronal and retrograde viral tracing shows multisynaptic pathways between the SCN and the adrenal glands (Buijs et al., 1999; Buijs et al., 2003). VIP and the $VPAC_2R$ are also expressed in the cortex of adrenal glands (Holzwarth, 1984; Cunningham and Holzwarth, 1989; Harmar et al., 2004), where the molecular oscillator is localized (Oster et al., 2006), and could well integrate downstream signals from the SCN.

In the present study, we were unable to detect diurnal rhythms in the adrenal expression of *Per1* and *Per2* transcripts, although the maintenance of the circadian *Per2* and *Bmal1* rhythms and the continuance of normal PER2::LUC rhythms suggest that the molecular oscillator is less affected in the adrenal glands than in the SCN of VIP KO mice. VIP-deficient mice lack rhythms in secreted ACTH and corticosterone (Loh et al., 2008), which could be due to a deficiency in SCN output signals or within the adrenal glands themselves. An intact molecular oscillator in the adrenal glands is necessary for interpretation of the rhythmic ACTH signal (Oster et al., 2006), and our finding that the molecular oscillator is relatively intact in VIP-deficient mice suggests a primary deficit in output from the SCN as opposed to an inability of the peripheral oscillators to respond to synchronization cues. The adrenal molecular oscillator, and subsequent secretion of corticosterone, is responsive to light (Ishida et al., 2005), and our findings that the adrenal *Per2* rhythms were worse in LD than in DD conditions raise the possibility that entrainment deficits are part of the problem. This is consistent with our previous data indicating that the photic regulation of *Per1* in the adrenals as well as the direct photic regulation of corticosterone is compromised in the VIP KO mice (Dragich et al., 2010).

The continuance of gene expression rhythms in the liver was surprising given the dependence of the liver molecular clockwork on rhythmic corticosterone and intact adrenal glands (Balsalobre et al., 2000; Oishi et al., 2005). Interestingly, all 3 rhythms in VIP-deficient liver *Per1*, *Per2*, and *Bmal1* were phase advanced compared to the WT controls. This finding was also reflected in the altered phase relationship of the VIP KO liver to the SCN using PER2::LUC monitoring. In contrast, the rhythms looked relatively normal in DD. Recent work suggests that scheduled feeding can be a powerful synchronizer of the circadian clock in the liver (Vollmers et al., 2009). A weakened SCN output in the VIP-deficient mice could well result in a greater role for nonphotic input in the synchronization of peripheral oscillators, as has been suggested in the case of $VPAC_2R$-deficient mice (Sheward et al., 2007; Hartley et al., 2009; Power et al., 2010). It may be that the liver clock in the VIP-deficient mice is better able to lock on to other cues in the absence of a strong signal from the SCN.

In summary, our data indicate that the loss of VIP results in the loss of rhythms in SCN expression of *Per1* and *Bmal1* while *Per2* continues to oscillate with greatly reduced amplitude. The simplest explanation for the loss of rhythmicity seen at the level of the SCN population is that the single cells continue to oscillate but have lost their temporal coordination. In addition, there is evidence that a certain percentage of SCN neurons lose their ability to generate circadian oscillations without VIP (Aton et al., 2005; Hughes et al., 2008). The peptide GRP appears to have some ability to compensate for the loss of VIP (Brown et al., 2005), and it may well be that multiple peptides normally work in concert to couple SCN oscillators. Besides its role as an intercellular synchronizing agent within the SCN (Vasalou et al., 2009), VIP is also likely to be involved in communicating circadian output to extra-SCN oscillators. Anatomically, at least some of the axons leaving the SCN express VIP, and many of the downstream targets express the $VPAC_2$Rs (Hermes et al., 2009). Our data indicate that the peripheral oscillators in the adrenals and liver are also affected by the loss of VIP. At least some of these effects are seen when the adrenals and liver were isolated from the SCN and cannot be a direct consequence of SCN dysfunction. The gene expression rhythms were most disrupted under LD conditions and relatively less so under DD conditions. In this regard, the VIP-mutant mice represent an interesting case in which the molecular clockworks are broken or misaligned in LD conditions. This type of misalignment is starting to be seen as a common symptom in psychiatric and neurological disorders (Wulff et al., 2010), and the VIP- and $VPAC_2$R-deficient mice represent interesting models to explore the impact of circadian misalignment on health.

Acknowledgments

We thank Donna Crandall for her assistance with preparation of the figures. We also thank UCLA undergraduates Sei Tateyama, Jacqueline Nguyen, and Julien Nguyen for their assistance with the ISH procedures. This research was supported by NIH grants NS-043169 and HL84240 to C.S.C., MH-65497 to J.A.W., and NS-043169 to J.M.D.

REFERENCES

Aton S, Block G, Tei H, Yamazaki S, Herzog E. Plasticity of circadian behavior and the suprachiasmatic nucleus following exposure to non-24-hour light cycles. J Biol Rhythms. 2004; 19:198–207. [PubMed: 15155006]

Aton S, Colwell C, Harmar A, Waschek J, Herzog E. Vasoactive intestinal polypeptide mediates circadian rhythmicity and synchrony in mammalian clock neurons. Nat Neurosci. 2005; 8:476–483. [PubMed: 15750589]

Balsalobre A, Brown S, Marcacci L, Tronche F, Kellendonk C, Reichardt H, Schütz G, Schibler U. Resetting of circadian time in peripheral tissues by glucocorticoid signaling. Science. 2000; 289:2344–2347. [PubMed: 11009419]

Brown S, Kunz D, Dumas A, Westermark P, Vanselow K, Tilmann-Wahnschaffe A, Herzel H, Kramer A. Molecular insights into human daily behavior. Proc Natl Acad Sci U S A. 2008; 105:1602–1607. [PubMed: 18227513]

Brown T, Hughes A, Piggins H. Gastrin-releasing peptide promotes suprachiasmatic nuclei cellular rhythmicity in the absence of vasoactive intestinal polypeptide-VPAC2 receptor signaling. J Neurosci. 2005; 25:11155–11164. [PubMed: 16319315]

Brown T, Colwell C, Waschek J, Piggins H. Disrupted neuronal activity rhythms in the suprachiasmatic nuclei of vasoactive intestinal polypeptide-deficient mice. J Neurophysiol. 2007; 97:2553–2558. [PubMed: 17151217]

Buijs R, Wortel J, Van Heerikhuize J, Feenstra M, Ter Horst G, Romijn H, Kalsbeek A. Anatomical and functional demonstration of a multisynaptic suprachiasmatic nucleus adrenal (cortex) pathway. Eur J Neurosci. 1999; 11:1535–1544. [PubMed: 10215906]

Buijs R, la Fleur S, Wortel J, Van Heyningen C, Zuiddam L, Mettenleiter T, Kalsbeek A, Nagai K, Niijima A. The suprachiasmatic nucleus balances sympathetic and parasympathetic output to

peripheral organs through separate preautonomic neurons. J Comp Neurol. 2003; 464:36–48. [PubMed: 12866127]

Ciarleglio C, Gamble K, Axley J, Strauss B, Cohen J, Colwell C, McMahon D. Population encoding by circadian clock neurons organizes circadian behavior. J Neurosci. 2009; 29:1670–1676. [PubMed: 19211874]

Colwell C, Michel S, Itri J, Rodriguez W, Tam J, Lelievre V, Hu Z, Liu X, Waschek J. Disrupted circadian rhythms in VIP- and PHI-deficient mice. Am J Physiol Regul Integr Comp Physiol. 2003; 285:R939–R949. [PubMed: 12855416]

Cunningham LA, Holzwarth MA. Autoradiographic distribution of 125I-VIP binding in the rat adrenal cortex. Peptides. 1989; 10:1105–1108. [PubMed: 2558364]

Dibner C, Schibler U, Albrecht U. The mammalian circadian timing system: organization and coordination of central and peripheral clocks. Annu Rev Physiol. 2010; 72:517–549. [PubMed: 20148687]

Dragich J, Loh D, Wang L, Vosko A, Kudo T, Nakamura T, Odom I, Tateyama S, Hagopian A, Waschek J, Colwell C. The role of the neuropeptides PACAP and VIP in the photic regulation of gene expression in the suprachiasmatic nucleus. Eur J Neurosci. 2010; 31:864–875. [PubMed: 20180841]

Guo H, Brewer J, Champhekar A, Harris R, Bittman E. Differential control of peripheral circadian rhythms by suprachiasmatic-dependent neural signals. Proc Natl Acad Sci U S A. 2005; 102:3111–3116. [PubMed: 15710878]

Harmar A, Sheward W, Morrison C, Waser B, Gugger M, Reubi J. Distribution of the VPAC2 receptor in peripheral tissues of the mouse. Endocrinology. 2004; 145:1203–1210. [PubMed: 14617572]

Harmar A, Marston H, Shen S, Spratt C, West K, Sheward W, Morrison C, Dorin J, Piggins H, Reubi J, et al. The VPAC(2) receptor is essential for circadian function in the mouse suprachiasmatic nuclei. Cell. 2002; 109:497–508. [PubMed: 12086606]

Hartley P, Sheward J, Scholefield E, French K, Horn J, Holmes M, Harmar A. Timed feeding of mice modulates light-entrained circadian rhythms of reticulated platelet abundance and plasma thrombopoietin and affects gene expression in megakaryocytes. Br J Haematol. 2009; 146:185–192. [PubMed: 19438469]

Hastings M, Reddy A, Maywood E. A clockwork web: circadian timing in brain and periphery, in health and disease. Nat Rev Neurosci. 2003; 4:649–661. [PubMed: 12894240]

Hermes M, Kolaj M, Doroshenko P, Coderre E, Renaud L. Effects of VPAC2 receptor activation on membrane excitability and GABAergic transmission in subparaventricular zone neurons targeted by suprachiasmatic nucleus. J Neurophysiol. 2009; 102:1834–1842. [PubMed: 19571188]

Holzwarth MA. The distribution of vasoactive intestinal peptide in the rat adrenal cortex and medulla. J Auton Nerv Syst. 1984; 11:269–283. [PubMed: 6392399]

Hughes A, Guilding C, Lennox L, Samuels R, McMahon D, Piggins H. Live imaging of altered period1 expression in the suprachiasmatic nuclei of Vipr2−/− mice. J Neurochem. 2008; 106:1646–1657. [PubMed: 18554318]

Ishida A, Mutoh T, Ueyama T, Bando H, Masubuchi S, Nakahara D, Tsujimoto G, Okamura H. Light activates the adrenal gland: timing of gene expression and glucocorticoid release. Cell Metab. 2005; 2:297–307. [PubMed: 16271530]

Kalló I, Kalamatianos T, Piggins H, Coen C. Ageing and the diurnal expression of mRNAs for vaso-active intestinal peptide and for the VPAC2 and PAC1 receptors in the suprachiasmatic nucleus of male rats. J Neuroendocrinol. 2004; 16:758–766. [PubMed: 15344914]

Kalsbeek A, Palm I, La Fleur S, Scheer F, Perreau-Lenz S, Ruiter M, Kreier F, Cailotto C, Buijs R. SCN outputs and the hypothalamic balance of life. J Biol Rhythms. 2006; 21:458–469. [PubMed: 17107936]

Liu A, Welsh D, Ko C, Tran H, Zhang E, Priest A, Buhr E, Singer O, Meeker K, Verma I, et al. Intercellular coupling confers robustness against mutations in the SCN circadian clock network. Cell. 2007; 129:605–616. [PubMed: 17482552]

Loh D, Abad C, Colwell C, Waschek J. Vasoactive intestinal peptide is critical for circadian regulation of glucocorticoids. Neuroendocrinology. 2008; 88:246–255. [PubMed: 18562786]

Maywood E, Reddy A, Wong G, O'Neill J, O'Brien J, McMahon D, Harmar A, Okamura H, Hastings M. Synchronization and maintenance of timekeeping in suprachiasmatic circadian clock cells by neuropeptidergic signaling. Curr Biol. 2006; 16:599–605. [PubMed: 16546085]

McDearmon E, Patel K, Ko C, Walisser J, Schook A, Chong J, Wilsbacher L, Song E, Hong H, Bradfield C, Takahashi J. Dissecting the functions of the mammalian clock protein BMAL1 by tissue-specific rescue in mice. Science. 2006; 314:1304–1308. [PubMed: 17124323]

Mezey E, Kiss J. Vasoactive intestinal peptide-containing neurons in the paraventricular nucleus may participate in regulating prolactin secretion. Proc Natl Acad Sci U S A. 1985; 82:245–247. [PubMed: 3881755]

Moore R, Eichler V. Loss of a circadian adrenal corticosterone rhythm following suprachiasmatic lesions in the rat. Brain Res. 1972; 42:201–206. [PubMed: 5047187]

Oishi K, Amagai N, Shirai H, Kadota K, Ohkura N, Ishida N. Genome-wide expression analysis reveals 100 adrenal gland-dependent circadian genes in the mouse liver. DNA Res. 2005; 12:191–202. [PubMed: 16303750]

Oster H, Damerow S, Kiessling S, Jakubcakova V, Abraham D, Tian J, Hoffmann MW, Eichele G. The circadian rhythm of glucocorticoids is regulated by a gating mechanism residing in the adrenal cortical clock. Cell Metab. 2006; 4:163–173. [PubMed: 16890544]

Piggins H, Cutler D. The roles of vasoactive intestinal polypeptide in the mammalian circadian clock. J Endocrinol. 2003; 177:7–15. [PubMed: 12697032]

Power A, Hughes A, Samuels R, Piggins H. Rhythm-promoting actions of exercise in mice with deficient neuropeptide signaling. J Biol Rhythms. 2010; 25:235–246. [PubMed: 20679493]

Schroeder A, Loh D, Jordan M, Roos K, Colwell C. Circadian regulation of cardiovascular function: a role for vasoactive intestinal peptide. Am J Physiol Heart Circ Physiol. 2011; 300:H241–H250. [PubMed: 20952671]

Sheward W, Maywood E, French K, Horn J, Hastings M, Seckl J, Holmes M, Harmar A. Entrainment to feeding but not to light: circadian phenotype of VPAC2 receptor-null mice. J Neurosci. 2007; 27:4351–4358. [PubMed: 17442819]

Teclemariam-Mesbah R, Kalsbeek A, Pevet P, Buijs R. Direct vasoactive intestinal polypeptide-containing projection from the suprachiasmatic nucleus to spinal projecting hypothalamic paraventricular neurons. Brain Res. 1997; 748:71–76. [PubMed: 9067446]

Vasalou C, Herzog E, Henson M. Small-world network models of intercellular coupling predict enhanced synchronization in the suprachiasmatic nucleus. J Biol Rhythms. 2009; 24:243–254. [PubMed: 19465701]

Vitaterna M, Ko C, Chang A, Buhr E, Fruechte E, Schook A, Antoch M, Turek F, Takahashi J. The mouse Clock mutation reduces circadian pacemaker amplitude and enhances efficacy of resetting stimuli and phase-response curve amplitude. Proc Natl Acad Sci U S A. 2006; 103:9327–9332. [PubMed: 16754844]

Vollmers C, Gill S, DiTacchio L, Pulivarthy S, Le H, Panda S. Time of feeding and the intrinsic circadian clock drive rhythms in hepatic gene expression. Proc Natl Acad Sci U S A. 2009; 106:21453–21458. [PubMed: 19940241]

Vosko A, Schroeder A, Loh D, Colwell C. Vasoactive intestinal peptide and the mammalian circadian system. Gen Comp Endocrinol. 2007; 152:165–175. [PubMed: 17572414]

Wang L, Dragich J, Kudo T, Odom I, Welsh D, O'Dell T, Colwell C. Expression of the circadian clock gene Period2 in the hippocampus: possible implications for synaptic plasticity and learned behaviour. ASN Neuro. 2009; 1:e00012. [PubMed: 19570032]

Webb AB, Angelo N, Huettner JE, Herzog ED. Intrinsic, nondeterministic circadian rhythm generation in identified mammalian neurons. Proc Natl Acad Sci U S A. 2009; 106:16493–16498. [PubMed: 19805326]

Welsh D, Takahashi J, Kay S. Suprachiasmatic nucleus: cell autonomy and network properties. Annu Rev Physiol. 2010; 72:551–577. [PubMed: 20148688]

Wulff K, Gatti S, Wettstein J, Foster R. Sleep and circadian rhythm disruption in psychiatric and neurodegenerative disease. Nat Rev Neurosci. 2010; 11:589–599. [PubMed: 20631712]

Yamaguchi S, Isejima H, Matsuo T, Okura R, Yagita K, Kobayashi M, Okamura H. Synchronization of cellular clocks in the suprachiasmatic nucleus. Science. 2003; 302:1408–1412. [PubMed: 14631044]

Yamazaki S, Takahashi J. Real-time luminescence reporting of circadian gene expression in mammals. Methods Enzymol. 2005; 393:288–301. [PubMed: 15817295]

Yoo S, Yamazaki S, Lowrey P, Shimomura K, Ko C, Buhr E, Siepka S, Hong H, Oh W, Yoo O, et al. PERIOD2::LUCIFERASE real-time reporting of circadian dynamics reveals persistent circadian oscillations in mouse peripheral tissues. Proc Natl Acad Sci U S A. 2004; 101:5339–5346. [PubMed: 14963227]

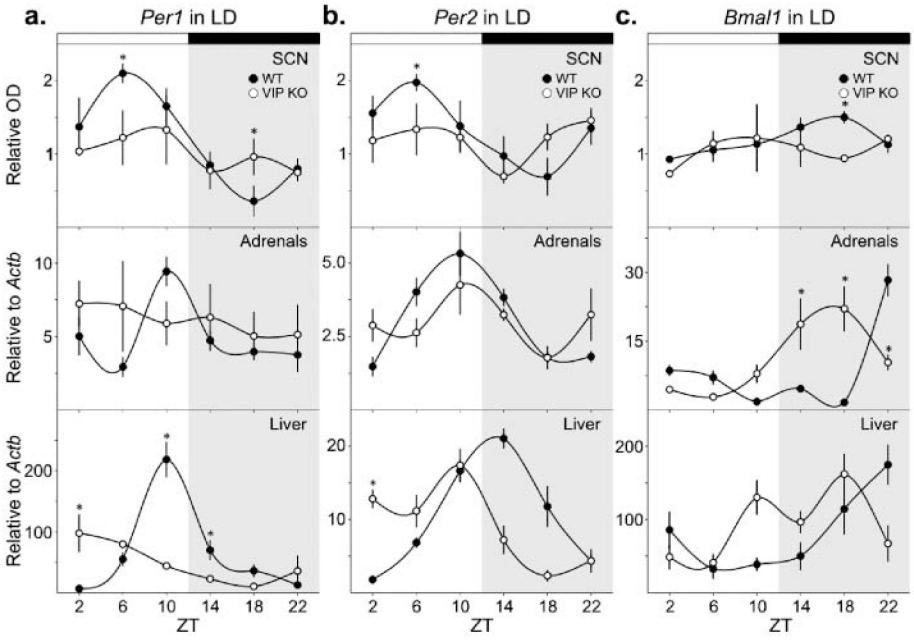

Figure 1.

Diurnal expression patterns of circadian genes in the SCN, adrenal glands, and liver of WT and VIP KO mice. Rhythms in gene expression were determined by 1-way ANOVA (Table 1), and interactions between time and genotype were ascertained by 2-way ANOVA with post hoc determination of differences between genotypes at each time point (*). (a) *Per1* expression was determined at ZT 2, 6, 10, 14, 18, and 22 from mice housed under a 12:12 LD cycle by ISH in the SCN (top) and by RT-PCR in the adrenal glands (middle) and liver (bottom). (b) *Per2* expression in the SCN (top), adrenal glands (middle), and liver (bottom). (c) *Bmal1* expression in the SCN (top), adrenal glands (middle), and liver (bottom).

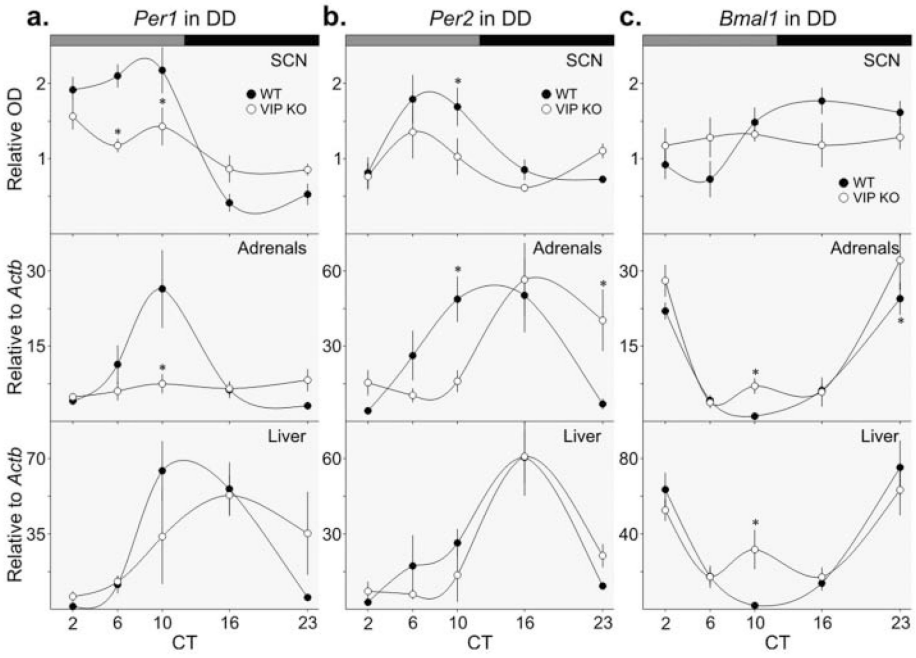

Figure 2.

Circadian expression patterns of circadian genes in the SCN, adrenal glands, and liver of WT and VIP KO mice. Rhythms in gene expression were determined by 1-way ANOVA (Table 2), and interactions between time and genotype were ascertained by 2-way ANOVA with post hoc determination of differences between genotypes at each time point (*). (a) *Per1* expression was determined at CT 2, 6, 10, 16, and 23 from mice housed for a minimum of 4 days under DD by ISH in the SCN (top) and by RT-PCR in the adrenal glands (middle) and liver (bottom). (b) *Per2* expression in the SCN (top), adrenal glands (middle), and liver (bottom). (c) *Bmal1* expression in the SCN (top), adrenal glands (middle), and liver (bottom).

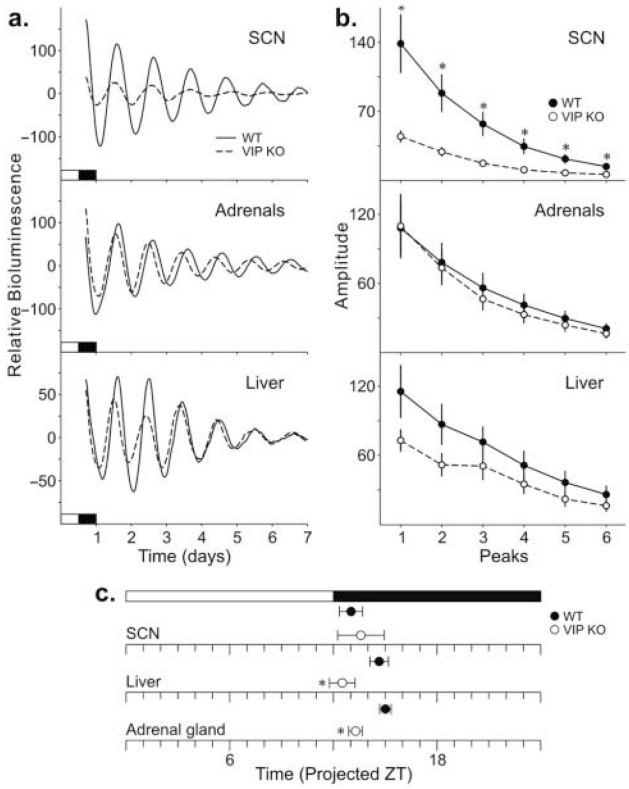

Figure 3.

PER2::LUC rhythms as measured by PMT over 10 days in the SCN, adrenal glands, and liver. (a) Typical examples of bioluminescence of WT (solid) and VIP KO (dashed) SCN (top), adrenal glands (middle), and liver (bottom) explants. (b) Amplitude of WT and VIP KO SCN (top), adrenal glands (middle), and liver (bottom) explants. (c) Phase relationship between WT and VIP KO SCN, adrenal glands, and liver explants as determined by the first peak measured. Significant differences between genotypes as determined by Student *t* tests (*).

Table 1

Diurnal rhythms in gene expression in WT and VIP-deficient mice.

Tissue	Gene	Genotype	Time v. Expression	Amplitude
SCN	*Per1*	WT	$F_{5,23} = 7.81$, $p < 0.001$	5.72 ± 0.21
		VIP KO	$F_{5,23} = 0.64$, $p = 0.67$	1.80 ± 0.37*
	Per2	WT	$F_{5,23} = 3.15$, $p = 0.032$	2.86 ± 0.15
		VIP KO	$F_{5,23} = 1.21$, $p = 0.34$	2.10 ± 0.21*
	Bmal1	WT	$F_{5,17} = 4.09$, $p = 0.02$	1.62 ± 0.05
		VIP KO	$F_{5,17} = 0.67$, $p = 0.66$	1.49 ± 0.21
Adrenal glands	*Per1*	WT	$F_{5,22} = 6.06$, $p = 0.002$	3.22 ± 0.34
		VIP KO	$F_{5,23} = 0.20$, $p = 0.96$	1.44 ± 0.31*
	Per2	WT	$F_{5,23} = 13.73$, $p < 0.001$	3.60 ± 0.51
		VIP KO	$F_{5,22} = 1.52$, $p = 0.24$	2.25 ± 0.43*
	Bmal1	WT	$F_{5,23} = 35.71$, $p < 0.001$	15.55 ± 1.95
		VIP KO	$F_{5,23} = 5.68$, $p = 0.003$	7.77 ± 1.73*
Liver	*Per1*	WT	$F_{5,23} = 27.12$, $p < 0.001$	30.94 ± 4.09
		VIP KO	$F_{5,23} = 3.99$, $p = 0.013$	9.16 ± 2.92*
	Per2	WT	$F_{5,23} = 24.75$, $p < 0.001$	11.57 ± 1.49
		VIP KO	$F_{5,22} = 9.70$, $p < 0.001$	7.39 ± 1.95*
	Bmal1	WT	$F_{5,23} = 5.52$, $p = 0.003$	6.11 ± 3.72
		VIP KO	$F_{5,22} = 5.21$, $p = 0.004$	3.32 ± 0.84

One-way ANOVA comparisons of time versus expression within genotypes are reported, along with the peak-to-trough amplitude for each gene.

* $p < 0.05$.

Table 2

Circadian rhythms in gene expression in WT and VIP-deficient mice.

Tissue	Gene	Genotype	Time v. Expression	Amplitude
SCN	*Per1*	WT	$F_{4,19} = 21.09$, $p < 0.001$	5.08 ± 0.37
		VIP KO	$F_{4,19} = 3.66$, $p = 0.04$	1.83 ± 0.21*
	Per2	WT	$F_{4,25} = 5.17$, $p = 0.005$	2.47 ± 0.44
		VIP KO	$F_{4,19} = 1.98$, $p = 0.15$	2.21 ± 0.58
	Bmal1	WT	$F_{4,25} = 5.05$, $p = 0.005$	2.43 ± 0.24
		VIP KO	$F_{4,19} = 0.18$, $p = 0.68$	1.14 ± 0.08*
Adrenal glands	*Per1*	WT	$F_{4,27} = 4.46$, $p = 0.008$	8.50 ± 2.50
		VIP KO	$F_{4,25} = 0.64$, $p = 0.64$	1.69 ± 0.46*
	Per2	WT	$F_{4,28} = 6.15$, $p = 0.001$	11.65 ± 2.17
		VIP KO	$F_{4,24} = 4.95$, $p = 0.006$	5.44 ± 1.41
	Bmal1	WT	$F_{4,28} = 45.81$, $p < 0.001$	23.86 ± 3.15
		VIP KO	$F_{4,25} = 8.13$, $p < 0.001$	8.55 ± 1.56*
Liver	*Per1*	WT	$F_{4,25} = 10.45$, $p < 0.001$	11.84 ± 2.54
		VIP KO	$F_{4,19} = 2.65$, $p = 0.08$	9.02 ± 1.60
	Per2	WT	$F_{4,24} = 4.62$, $p = 0.008$	22.21 ± 9.31
		VIP KO	$F_{4,19} = 11.92$, $p < 0.001$	18.47 ± 3.20
	Bmal1	WT	$F_{4,24} = 17.93$, $p < 0.001$	39.11 ± 7.46
		VIP KO	$F_{4,19} = 9.01$, $p < 0.001$	1.99 ± 0.43*

One-way ANOVA comparisons of time versus expression within genotypes are reported, along with the peak-to-trough amplitude for each gene.

* $p < 0.05$.

Table 3

PER2::LUC bioluminescence parameters of WT and VIP KO ex vivo explants.

SCN	WT	VIP KO
Period (h)	24.87 ± 0.27	24.98 ± 0.42
Phase (ZT)	13.65 ± 0.58	14.22 ± 1.25
First amplitude	138.64 ± 77.94	44.58 ± 5.31**
Damping (d)	3.93 ± 0.15	4.26 ± 0.53
Variation in time interval between peaks	1.29 ± 0.26	2.56 ± 0.41*
Adrenal Glands	**WT**	**VIP KO**
Period (h)	22.85 ± 0.50	23.03 ± 0.40
Phase (ZT)	15.51 ± 0.25	13.84 ± 0.35**
First amplitude	108.04 ± 21.40	109.79 ± 24.44
Damping (d)	4.63 ± 0.22	4.14 ± 0.14
Variation in time interval between peaks	0.64 ± 0.08	0.68 ± 0.11
Liver	**WT**	**VIP KO**
Period (h)	24.91 ± 0.26	24.92 ± 0.42
Phase (ZT)	15.28 ± 0.47	13.16 ± 0.70*
First amplitude	115.41 ± 21.25	72.89 ± 8.85
Damping (d)	6.04 ± 0.93	5.90 ± 1.40
Variation in time interval between peaks	1.74 ± 0.14	2.32 ± 0.17*

* $p < 0.05$;

** $p < 0.01$.